View metadata, citation and similar papers at core.ac.uk

brought to you by CORE

provided by Carolina Digital Repository

THE JOURNAL OF BIOLOGICAL CHEMISTRY VOL. 285, NO. 45, pp. 34939–34949, November 5, 2010
© 2010 by The American Society for Biochemistry and Molecular Biology, Inc. Printed in the U.S.A.

Human Alveolar Type II Cells Secrete and Absorb Liquid in Response to Local Nucleotide Signaling*[S]

Received for publication, July 12, 2010, and in revised form, August 23, 2010 Published, JBC Papers in Press, August 27, 2010, DOI 10.1074/jbc.M110.162933

Peter F. Bove, Barbara R. Grubb, Seiko F. Okada, Carla M. P. Ribeiro, Troy D. Rogers, Scott H. Randell, Wanda K. O'Neal, and Richard C. Boucher[1]

From the Department of Medicine, Cystic Fibrosis/Pulmonary Research and Treatment Center, University of North Carolina at Chapel Hill, Chapel Hill, North Carolina 27599

A balance sheet describing the integrated homeostasis of secretion, absorption, and surface movement of liquids on pulmonary surfaces has remained elusive. It remains unclear whether the alveolus exhibits an intra-alveolar ion/liquid transport physiology or whether it secretes ions/liquid that may communicate with airway surfaces. Studies employing isolated human alveolar type II (AT2) cells were utilized to investigate this question. Human AT2 cells exhibited both epithelial Na^+ channel-mediated Na^+ absorption and cystic fibrosis transmembrane conductance regulator-mediated Cl^- secretion, both significantly regulated by extracellular nucleotides. In addition, we observed in normal AT2 cells an absence of cystic fibrosis transmembrane conductance regulator regulation of epithelial Na^+ channel activity and an absence of expression/activity of reported calcium-activated chloride channels (TMEM16A, Bestrophin-1, ClC2, and SLC26A9), both features strikingly different from normal airway epithelial cells. Measurements of alveolar surface liquid volume revealed that normal AT2 cells: 1) achieved an extracellular nucleotide concentration-dependent steady state alveolar surface liquid height of ~4 μm *in vitro*; 2) absorbed liquid when the lumen was flooded; and 3) secreted liquid when treated with UTP or forskolin or subjected to cyclic compressive stresses mimicking tidal breathing. Collectively, our studies suggest that human AT2 cells *in vitro* have the capacity to absorb or secrete liquid in response to local alveolar conditions.

The thin liquid layer lining the alveolar space is essential for maintaining efficient gas exchange, surfactant homeostasis, and defense against inhaled toxins/pathogens. Airway epithelial cells actively secrete or absorb ions in response to local stimuli to coordinately regulate the liquid layer lining airway surfaces (1, 2). However, it remains unclear whether the alveolar epithelium exhibits similar capacities and, if so, how the physiologies of the two regions are coordinated.

The alveolar surface consists of two main cell types, alveolar type I (AT1)[2] and alveolar type II (AT2) cells. AT1 cells are large thin cells that cover a large part of the alveolar surface area. AT2 cells are cuboidal in shape and comprise 5% of the alveolar surface area, yet they constitute 60% of alveolar epithelial cells (3–6). Because AT2 cells can be isolated, cultured, and studied *in vitro*, they have been used in attempts to understand their contribution to alveolar liquid balance.

AT2 cells express the Na^+ and Cl^- transport pathways required to mediate liquid homeostasis on the alveolar surface. Na^+ uptake occurs at the apical surface of rat AT2 cells in large part through the amiloride-sensitive epithelial Na^+ channel (ENaC) (7–9), and *in situ* hybridization studies have identified the presence of mRNA for all three subunits of ENaC in rat alveolar cells (8, 9). Na^+ entering via ENaC is pumped out of the cell into the interstitium by the ouabain-sensitive Na^+,K^+-ATPase pump (7, 10). *In vitro* Ussing chamber studies have identified ENaC-mediated Na^+ absorption across rat AT2 cell monolayers, and amiloride-sensitive whole lung liquid absorption has been detected in several species *in vivo* (11, 12).

Although numerous studies have established active Na^+ transport as a major pathway for regulating liquid transport across the alveolar epithelium, the role of Cl^- transport pathways, involving the cystic fibrosis transmembrane conductance regulator (CFTR), is unresolved. AT2 cells express CFTR mRNA, protein, and channels (13–15). Experiments in wild-type mice and the *ex vivo* human lungs demonstrated that liquid absorption was inhibited by glibenclamide, suggesting a role for CFTR-dependent Cl^- absorption (13, 14). Moreover, both liquid absorption and Cl^- uptake from the distal airspace were stimulated by β-agonists in wild-type mice but not in ΔF508 CFTR mutant mice (16). In contrast, evidence for alveolar liquid secretion was demonstrated by confocal microscopy in mice, which was blunted by the CFTR inhibitor ($CFTR_{inh}$-172) and was absent in $CFTR^{(-/-)}$ mice, suggesting that the murine alveolar epithelium secrete liquid via CFTR. Thus, a challenge remains to understand the relative roles of CFTR-mediated Cl^- absorption *versus* secretion within the alveolar space.

* This work was supported, in whole or in part, by National Institutes of Health Grants HL34322, 2P30DK065988, and P50HL084934. This work was also supported by Cystic Fibrosis Foundation Grant RDP R026-CR07.

[S] The on-line version of this article (available at http://www.jbc.org) contains supplemental Table S1.

[1] To whom correspondence should be addressed: Cystic Fibrosis/Pulmonary Research and Treatment Center, University of North Carolina at Chapel Hill, 7011 Thurston-Bowles Bldg., 96 Manning Dr., Chapel Hill, NC 27599. Fax: 919-966-5178; E-mail: R_Boucher@med.unc.edu.

[2] The abbreviations used are: AT, alveolar type; CF, cystic fibrosis; SP-C, surfactant protein-C; CFTR, cystic fibrosis transmembrane conductance regulator; ENaC, epithelial sodium channel; ASL, airway surface liquid; AvSL, alveolar surface liquid; CCS, cyclic compressive stress; PD, potential difference; CaCC, Ca^{2+}-activated chloride channel; DIDS, 4,4′-diisothiocyanostilbene-2,2′-disulfonic acid.

Coordinate regulation of Na^+ absorption and Cl^- secretion in airway epithelia is mediated in part via the concentrations of nucleotides/nucleosides in the luminal extracellular compartment (17). For example, ATP mediates regulatory responses via $P2Y_2$ receptor stimulation, and ATP metabolism provides a source of adenosine for stimulation of the A_{2b} adenosine receptor (18–20). Recently, the mechanical stresses associated with tidal breathing have been shown to stimulate luminal nucleotide release from airway epithelial cells, providing a link between local stresses and regulation of airway surface liquid (ASL) volume (21). Similarly, purinergic signaling may contribute to the integrated control of ion/liquid homeostasis within the alveolar space. Nucleotide receptors and adenosine receptors (12, 22) have been identified in mouse and rat AT2 cells, and ATP or UTP has been reported to regulate Na^+ and Cl^- transport in cultured rat AT2 cells (23, 24). Whether a role for nucleotide release in response to the mechanical stresses of tidal breathing plays a role in regulating human alveolar liquid homeostasis is as yet unknown.

In this study, we investigated the regulation of alveolar surface liquid (AvSL) volume, utilizing *in vitro* techniques. First, we identified the pathways that mediate Na^+ absorption and Cl^- secretion with electrophysiologic techniques in cultured normal human AT2 cells. Second, we studied the integrated functions of ion transport via measuring the volume of the AvSL produced by cultured normal human AT2 cells under basal and stimulated conditions with confocal microscopy.

EXPERIMENTAL PROCEDURES

Alveolar Type II Cell Isolation—Normal lungs rejected for transplant by local and distant organ procurement agencies received by the University of North Carolina Cystic Fibrosis Center Tissue Culture Core were studied following protocols approved by the University of North Carolina Institutional Review Board. Human AT2 cells were isolated as previously described with slight modifications (25). The right middle lobe was selected, cannulated through the main stem bronchus, and removed from the rest of the lung. The distal airspaces were lavaged 10 times using a Ca^{2+}- and Mg^{2+}-free solution containing 0.5 mM EGTA (Sigma), 140 mM NaCl (Fisher), 5 mM KCl (Sigma), 2.5 mM Na_2HPO_4 (Fisher), 10 mM HEPES (Sigma), and 6 mM glucose (Sigma) and then lavaged three times using the solution above with no glucose but adding 2.0 mM $CaCl_2$ (Sigma) and 1.3 mM $MgSO_4$ (Sigma). Elastase (Worthington, Lakewood, NJ), 13 units/ml in the Ca^{2+}- and Mg^{2+}-containing solution above, was instilled into the distal airspaces, and the lobe was incubated at 37 °C for 45 min. Following digestion, the lobe was minced finely in the presence of 5% FBS (Atlanta Biological, Lawrenceville, GA) and DNase (Sigma) at 500 μg/ml. The suspension was filtered sequentially through two layers of sterile gauze, followed by filtration through 150- and 40-μm sterile nylon meshes (Small Parts, Miramar, FL). The filtrate was spun at 130 × *g* for 10 min at 4 °C. The cell pellet was resuspended in DMEM plus 10% FBS and decanted onto PBS- and DMEM-rinsed Petri dishes coated with a human IgG antibody (500 μg/ml in Tris buffer, pH 9.5) (Sigma) against macrophages for 90 min at 37 °C. The nonadherent AT2 cells were collected, spun at 130 × *g* for 10 min, and resuspended in DMEM plus 10% FBS. The final AT2 suspension was seeded on rat tail collagen I-coated (250 μg/ml; Sigma) 1.12-cm^2 inserts (Fisher; Corning 3460), in 5% CO_2 at 37 °C at a concentration of 1.0×10^6 cells/insert. The cells were maintained in DMEM, 10% FBS with penicillin, streptomycin, gentamicin, and amphotericin. For the first 5 days of culture, the medium was supplemented with ceftazidime, tobramycin, and vancomycin (all cultures). The culture medium was changed 48 h after seeding. 72 h after isolation, the AT2 cells were washed once with PBS, and culture medium was added only to the basolateral side of the insert. All of the experiments were performed 4–9 days after seeding.

RT-PCR Analysis—Total RNA was extracted using TRI Reagent (Sigma) according to the manufacturer's protocol for every sample. Reverse transcription was performed using 2–5 μg of total RNA, and PCRs were performed using a GeneAmp PCR System 2,700 (Applied Biosystems, Foster City, CA). 40 cycles of PCR were performed. PCR products were resolved by 1% agarose gel electrophoresis and visualized by ethidium bromide staining. The expression of all genes of interest was normalized to that of GAPDH. Primer sequences can be found in supplemental Table 1 (S1).

Immunofluorescence Analysis—Freshly isolated suspensions (cytospins), cultured human AT2 cells (on rat tail type-I collagen coated inserts), and mouse whole lung tissue were fixed in 4% paraformaldehyde, PBS for 5 min, permeabilized using 0.1% Triton X-100, PBS, and blocked in 2% BSA, PBS, 0.1% Triton X-100 for 1 h. The cells were probed with antibodies against the precursor form of surfactant protein C (proSP-C; Chemicon, Temecula, CA), AQP-3 (Chemicon), AQP-5 (Chemicon), or CFTR (J. Riordan, monoclonal antibody UNC 528) in 0.1% Triton X-100, PBS for 1 h at 37 °C (or overnight at 4 °C). Negative controls used species-specific IgG. The sample(s) were washed three times with PBS and then incubated with a secondary antibody (Alexa-Fluor 568 goat anti-mouse/rabbit) (Invitrogen) in 0.1% Triton X-100, PBS for 1 h at 37 °C in the dark. The cell nuclei were stained with either DAPI (Anaspec, Fremont, CA) or SYTOX® Green (Invitrogen), and the slides were washed, mounted, and imaged using confocal microscopy.

Ion Transport Measurements—Ussing chamber studies were performed on human AT2 cultures under basal conditions or after the addition of designated reagents under open circuit conditions (27). Basal potential difference (PD) and changes in response to each added reagent were measured, and the equivalent short circuit (I_{eq}) was calculated as previously described (27, 28). The following agents were tested: amiloride (Sigma) (100 μM, luminal); forskolin (Sigma) (10 μM, luminal); UTP (GE Healthcare) (100 μM, luminal); ATP (GE Healthcare) (100 μM, luminal); adenosine (Sigma) (100 μM, luminal); UDP (Sigma), (100 μM, luminal); ionomycin (Sigma) (5 μM, luminal); or the CFTR inhibitor ($CFTR_{inh}$-172; (10 μM, luminal).

Measuring Intracellular Ca^{2+} ($[Ca^{2+}]_i$)—5–9-Day-old cultures of normal AT2 cells were loaded with 2.5 μM fura-2/AM and basal Ca^{2+} levels, and Ca^{2+} mobilization in response to 100 μM UTP followed by ionomycin (10 μM) was measured by microfluorimetry in the presence of a HEPES-buffered saline solution containing 1.3 mM Ca^{2+}, as previously described (29, 30). The data are expressed as Δ340/380 (UTP-induced peak value − base-line value) fura-2 fluorescence.

ATP Concentration and Release Rates—Real time basal ATP levels and release rates were performed as previously described (31). Confluent AT2 cells with soluble luciferase (Sigma; L9506; 0.5–2.0 μg/culture) and luciferin (150 μM) added to the mucosal surface (90 μl) were gently placed in the Turner TD-20/20 luminometer. Luminescence was measured every minute until the ALU values reached steady state, the measure of basal concentrations. ATP release rates from resting AT2 cells were measured by monitoring ATP accumulation in real time after maximal inhibition of cell surface nucleotidase activities. The nucleotidase inhibitor mixture contained 300 μM β,γ-methylene-ATP, 30 μM ebselen, and 10 mM levamisole to inhibit ecto-nucleotide pyrophosphatase/phosphodiesterases, ecto-nucleotide triphosphate diphosphohydrolases, and nonspecific alkaline phosphatases. After the basal ATP concentration was recorded as described above, the inhibitor mixture was added to the mucosal liquid, and ATP concentrations were measured every minute. In selected experiments, forskolin (10 μM) was added during the release measurements. A standard curve for each experiment was also generated using a solution of ATP (GE Healthcare; 100 mM).

Measuring AvSL Height—AT2 cultures, under air-liquid interface conditions, were incubated with CellTrace™ Calcein Green, AM (3 μM; Invitrogen) for 20 min at 37 °C to stain live cells. The cells were washed with PBS, followed by apical addition of Texas Red-labeled 70-kDa dextran/PBS (2.5 mg/ml; Invitrogen) to measure AvSL height. For studies of basal AvSL regulation, 25 μl of Texas Red-labeled 70-kDa dextran, dextran, PBS, and perflurocarbon (50 μl) were added, and the cells were imaged immediately and serially for 24 h at five predetermined sites, as previously described (32). Studies of forskolin or UTP were performed by incubating 25 μl of Texas Red-labeled 70-kDa dextran, PBS fluorophore on the cell surface for 30 min at 37 °C, followed by removal of excess dextran to initiate studies under steady state "thin film" conditions. The images were taken serially post-agonist addition with *x-z* confocal microscopy. In selected studies, apyrase (10 units/ml; Sigma) was added with the 70-kDa dextran, PBS solution for studies focused on: 1) control of basal AvSL height and 2) mechanisms of forskolin responses. For studies designed to measure inhibition of CFTR activity, the CFTR inhibitor ($CFTR_{inh}$-172) was added to the 70-kDa dextran, PBS solution, and cultures were incubated at 37 °C for 30 min, followed by the addition of forskolin or UTP.

Cyclic Compressive Stress (CCS)—25 μl of the Texas Red-labeled 70-kDa dextran, PBS fluorophore were added to the mucosal surface of AT2 cultures, and residual liquid was aspirated after 30 min, following which *x-z* confocal images were obtained at 0, 1, and 24 h under control conditions or under CCS (0–20 cmH_2O), delivered by a published technique (21). To explore the role of nucleotide release in CCS-mediated alveolar liquid responses, parallel AT2 cultures were treated with apyrase (10 units/ml; Sigma) in the 70-kDa dextran, PBS fluorophore for 30 min prior to the initiation of CCS.

Data Expression and Statistical Analysis—All of the experiments were performed in triplicate, and the cells were obtained from at least three different patient specimens. The data are presented as the means ± S.D., analyzed by one-way analysis of variance, and the differences were considered significant if $p < 0.05$ (*) and $p < 0.01$ (#).

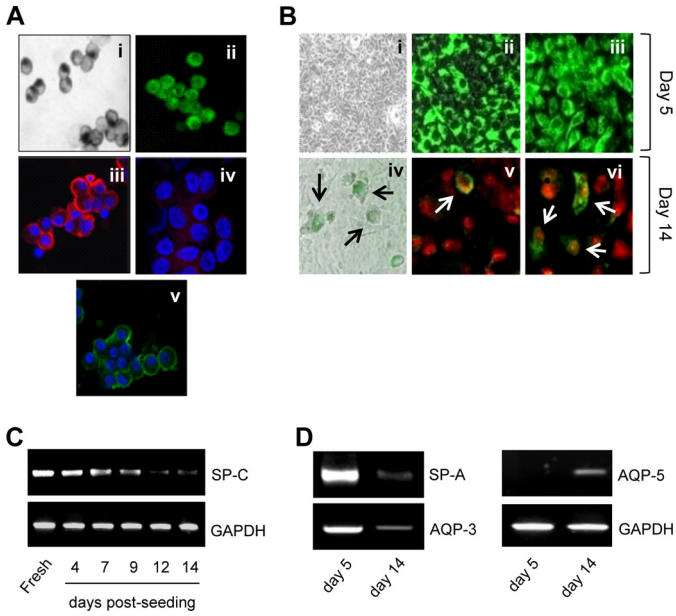

FIGURE 1. **Characterization of human AT2 cells.** *A*, the purity of freshly isolated normal human AT2 cells (*panel i*) was determined by immunostaining using a proSP-C antibody. Freshly isolated normal AT2 cells were also probed using Lysotracker® Green DND-26 (*panel ii*), antibodies probing for AQP-3 (*panel iii*), AQP-5 (*panel iv*), or CFTR (*panel v*) protein expression to assess AT2 purity. *B*, normal human AT2 cells were cultured in DMEM + 5% FBS medium on rat tail collagen-1-coated 1.12-cm^2 membrane Transwell inserts and exposed to air-liquid interface 96 h post-seeding. Differential interference contrast (*panel i*, 20× objective), Lysotracker® (*panel ii*), and proSP-C (*panel iii*) imaging were performed to assess the purity of AT2 cultures 5 days after seeding by confocal microscopy. Normal human AT2 cells 14 days in culture were probed using Lysotracker® (*panel iv*), proSP-C (*panel v*), or AQP-5 (*panel vi*) to assess the trans-differentiation process of AT2 cells in culture over time into AT1-like cells (*arrows* indicate positive cells). *C*, mRNA from freshly isolated human AT2 cells, as well as mRNA from cells 4–14 days post-seeding, were collected. SP-C gene expression was measured using semi-quantitative PCR. *D*, semi-quantitated PCR was also measured for SP-A, AQP-3, and AQP-5 gene expression in normal AT2 cultures 5 or 14 days after seeding to characterize cell phenotype. All of the original images were taken using a 63× objective, unless otherwise stated.

RESULTS

Characterization of Freshly Isolated and Cultured AT2 Cells—Following elastase digestion and filtration/enrichment, the purity of the final cell preparations was determined for human normal AT2 cells to be 91.7 ± 2.9% as assessed by immunostaining for proSP-C (normal; Fig. 1*A*, *panel i*). Freshly isolated cells also expressed other AT2 cell markers, including lamellar bodies imaged with the fluorescent probe Lysotracker® Green DND-26 (Lysotracker) (Fig. 1*A*, *panel ii*) and aquaporin-3 (AQP-3; Fig. 1*A*, *panel iii*), which was detected immunocytochemically. In contrast, preparations were negative for the AT1 cell marker aquaporin-5 (AQP-5; Fig. 1*A*, *panel iv*) (33), as assessed by immunostaining. CFTR protein was detected in freshly isolated normal AT2 preparations by immunostaining/confocal microscopy (Fig. 1*A*, *panel v*).

Normal human AT2 cells were seeded on rat tail type 1 collagen-coated polycarbonate filters and formed confluent monolayers within 96 h after seeding. Transepithelial resis-

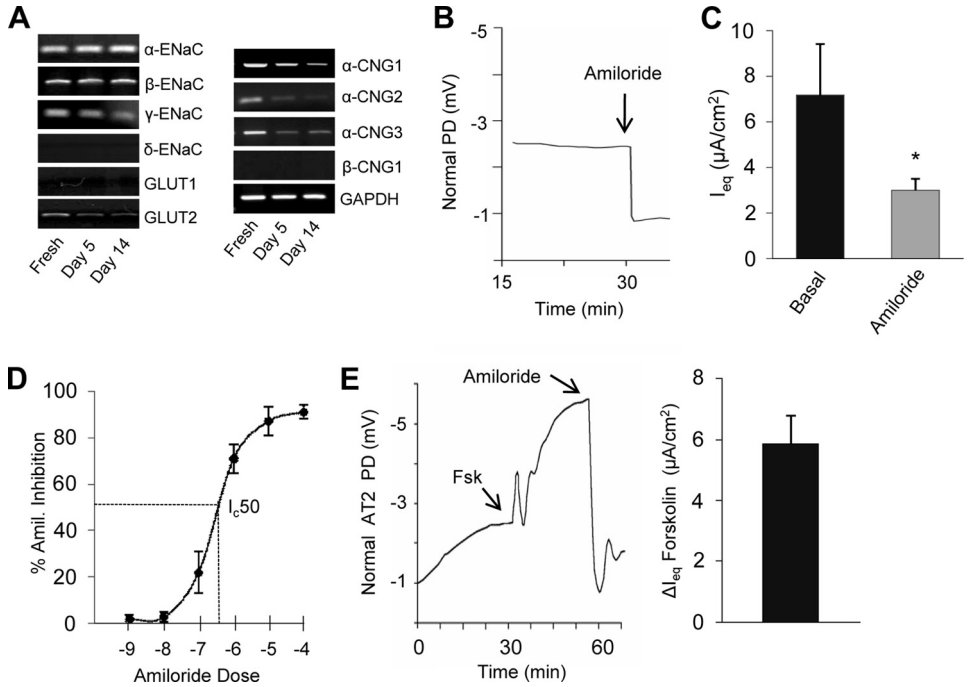

FIGURE 2. **Na^+ transport properties of human AT2 cells.** *A*, semi-quantitative PCR analysis was performed to identify the expression of genes whose products could mediate electrogenic Na^+ absorption in freshly isolated or cultured human AT2 cells. *B*, normal AT2 cultures were mounted in Ussing chambers, transepithelial electric PDs measured under open circuit conditions, with response to amiloride (100 μM, luminal). *C*, basal and amiloride-sensitive equivalent short circuit currents (I_{eq}) were measured in normal AT2 cultures mounted in Ussing chambers (means ± S.D.; $n \geq 6$; *, $p < 0.05$). *D*, an amiloride dose-response curve was generated in normal AT2 cultures (mean ± S.D.; $n \geq 3$). *E*, the potential difference (mV) and the change in equivalent short circuit current (ΔI_{eq}) were measured after exposure to forskolin (10 μM) followed by treatment with amiloride (100 μM, luminal) in normal AT2 cultures ($n \geq 6$).

tance was 419.3 Ω*cm^2 ± 168.1 at day 5 in culture ($n > 3$ different patient specimen codes). At day 5, the AT2 cell monolayers retained AT2-like features, as indexed by differential interference contrast microscopy (Fig. 1*B*, *panel i*), Lysotracker (Fig. 1*B*, *panel ii*), and proSP-C (Fig. 1*B*, *panel iii*) antibody immunostaining. To address the possibility that AT2 cells trans-differentiated in culture over time to an "AT1-like" cell phenotype, AT2 cells were probed over 14 days in culture with Lysotracker (Fig. 1*B*, *panel iv*), proSP-C (Fig. 1*B*, *panel v*), and AQP-5 antibodies (Fig. 1*B*, *panel vi*) and imaged by confocal microscopy. Cultures lost significant expression of the Lysotracker and pro-SPC with time. In contrast, AQP-5 expression increased, supporting the concept that AT2 trans-differentiation into AT1-like cells in culture has occurred by day 14.

Human AT2 mRNA was isolated from fresh preparations and cells 2–14 days in culture, and RT-PCR was performed to characterize the expression of SP-C mRNA over time (Fig. 1*C*). Expression of SP-C decreased with time in culture. SP-A, AQP-3, and AQP-5 mRNA was analyzed at 5 and 14 days in culture by RT-PCR to more fully characterize the AT2 culture phenotype (Fig. 1*D*). Overall, these studies confirmed the reduction of AT2 markers (SP-A, SP-C, and AQP-3) and revealed the appearance of an AT1 marker (AQP-5) over time in our cultures. Therefore, all of the experiments within this study were performed on AT2 cultures 4–9 days after seeding.

Na^+ Transport by AT2 Cells—To identify which sodium channels/subunits were expressed in human AT2 cells, semi-quantitative PCR analysis was performed on mRNA from freshly isolated and AT2 cells 5 or 14 days in culture. The α, β, and γ subunits of ENaC were expressed at all time points; however, no expression of the δ subunit was detected (Fig. 2*A*). With respect to other electrogenic Na^+ transporters, expression of the glucose-sodium transporter-2 (*GLUT2/SLC2A2*) was detected but not the glucose-sodium transporter-1 (*GLUT1/SLC2A1*) gene. In addition, mRNA expression of the α-cyclic nucleotide-gated Na^+ channels (α-CNG1–3) was detected, but no expression was observed of the β-CNG1 in AT2 cultures. Bioelectric measurements of normal and CF AT2 cultures revealed small inhibitory responses (<5%) to the glucose-sodium transporter inhibitor (phloridzin) or the cyclic nucleotide-gated sodium channel inhibitor (diltiazem) (<5%), suggesting that Na^+ transport in human AT2 cells is primarily mediated by ENaC. Therefore, we initiated experiments to further characterize ENaC-mediated Na^+ absorption in human AT2 cultures.

To measure basal ENaC-mediated Na^+ absorption, normal human AT2 cells were treated with amiloride (100 μM), and the change in PD was measured (Fig. 2*B*). The basal equivalent short circuit current (I_{eq}) and the post-amiloride-sensitive I_{eq} values were 7.69 ± 1.9 and 3.11 ± 0.52 μA/cm^2, respectively (Fig. 2*C*), suggesting that Na^+ absorption (Δamiloride I_{eq} = 4.58 μA/cm^2) is the dominant basal ion transport process. An amiloride dose-response curve for normal AT2 cultures revealed an IC_{50} of $\sim 5 \times 10^{-7}$ M (Fig. 2*D*).

Because agents that raise cellular cAMP levels increase Na^+ absorptive rates in mouse and rat AT2 cells (34), similar protocols were performed in human AT2 cells. Normal human AT2 cultures exposed to forskolin (10 μM) exhibited a rapid spike, followed by a slow gradual increase in PD that was inhibited by amiloride (Fig. 2*E*). The mean increase in Na^+ absorption stimulated by forskolin was ~6 μA·cm^2.

Cl^- Secretion by AT2 Cells—We first characterized cAMP-regulated/CFTR-mediated Cl^- secretion in AT2 cells in Ussing chambers. Normal human AT2 cultures were treated with $CFTR_{inh}$-172 (10 μM), a CFTR inhibitor (35), to measure the contribution of CFTR to basal I_{eq}, followed by exposure to amiloride (Fig. 3*A*). The change in I_{eq} in response to $CFTR_{inh}$-172 was small, ~0.4 μA/cm^2, suggesting that normal AT2 cells exhibit only a small rate of CFTR-mediated Cl^- secretion under basal conditions (Fig. 3*B*). To assess the capacity of CFTR to accelerate Cl^- secretion, human normal AT2 cultures were treated with forskolin in the presence of amiloride. Forskolin induced a rapid increase in the potential difference in AT2 cul-

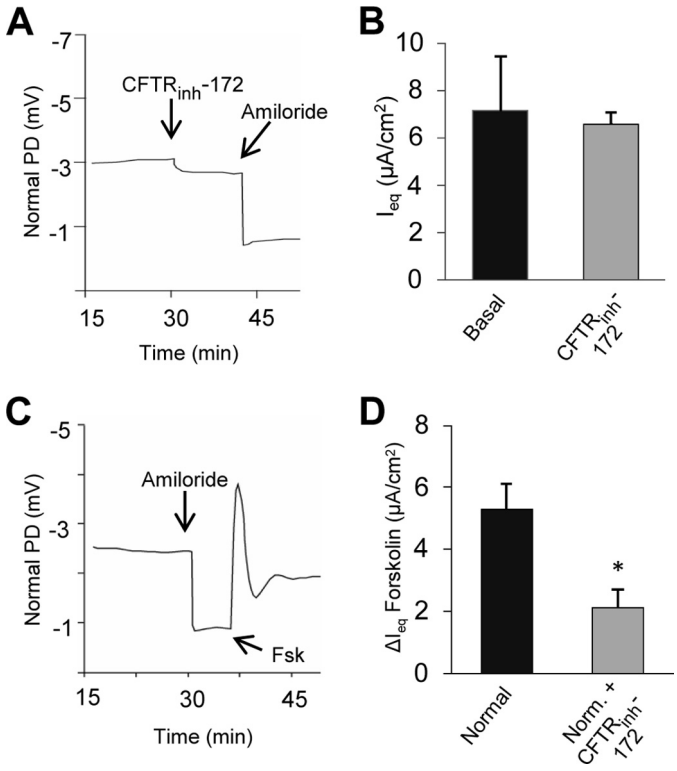

FIGURE 3. **Cl^- transport properties of human AT2 cells.** *A*, normal human AT2 cultures were studied under basal conditions and after exposure to the CFTR inhibitor ($CFTR_{inh}$-172, 10 μM) followed by the addition of amiloride (100 μM) in Ussing chambers. *B*, equivalent short circuit currents (I_{eq}) in normal AT2 cells under basal *versus* post-$CFTR_{inh}$-172 addition are summarized (means ± S.D.; $n \geq 6$). *C*, Ussing chamber studies were performed to measure the forskolin-mediated secretory capacity of normal AT2 cultures in the presence of amiloride. *D*, the change in the equivalent short circuit current (ΔI_{eq}) induced by forskolin in normal AT2 cultures, with or without $CFTR_{inh}$-172 (10 μM) (mean ± S.D.; $n \geq 6$; *, $p < 0$).

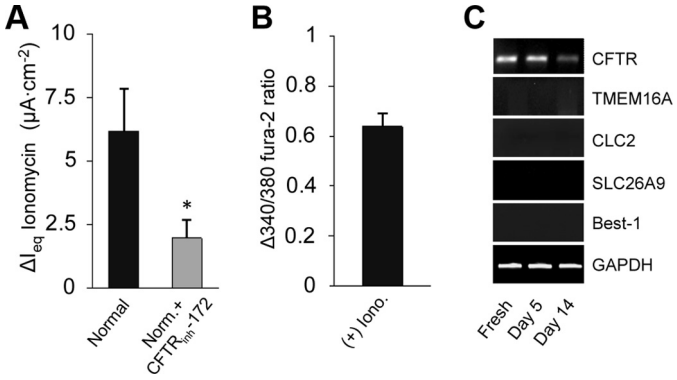

FIGURE 4. **Calcium-mediated Cl^- secretion in human AT2 cells.** *A*, the changes in equivalent short circuit currents (ΔI_{eq}) were measured and quantitated by Ussing chamber analysis in response to ionomycin (5 μM, luminal) in normal AT2 cells and normal AT2 cells pretreated with $CFTR_{inh}$-172 in the presence of amiloride (means ± S.D.; $n \geq 3$; *, $p < 0.05$). *B*, intracellular Ca^{2+} responses (Δ340/380 fura-2 ratio) of fura-loaded normal AT2 cells were measured, and the responses were summarized (means ± S.D.; $n \geq 3$). *C*, semi-quantitative PCR analysis was performed to identify chloride channel genes (CFTR, TMEM16A, CLC2, and SLC26A9) expressed in freshly isolated or cultured normal AT2 cells.

tures (Fig. 3*C*), consistent with anion (Cl^-) secretion. The acute anion secretory effects of forskolin were significantly blocked in normal AT2 cells pretreated with $CFTR_{inh}$-172 (Fig. 3*D*). These results suggest that forskolin-stimulated Cl^- secretion in amiloride-pretreated normal AT2 cells is predominantly mediated via CFTR.

We next measured $[Ca^{2+}]_i$-regulated Cl^- secretion in human AT2 cells. There was little change in basal I_{eq} in response to putative Ca^{2+}-activated chloride channel (CaCC) antagonists, *e.g.* DIDS or niflumic acid (data not shown). Increases in I_{eq} were observed when normal AT2 cultures were treated with the Ca^{2+} ionophore, ionomycin, in the presence of amiloride (Fig. 4*A*). DIDS or niflumic acid (general inhibitors of Ca^{2+}-activated chloride channels) did not block the ionomycin-induced currents in normal AT2 cultures (data not shown). Surprisingly, the acute response to ionomycin was significantly inhibited in normal AT2 cultures pretreated with $CFTR_{inh}$-172 (Fig. 4*A*). These data indicate that CFTR mediates $[Ca^{2+}]_i$-regulated anion secretion in normal human AT2 cells.

We performed two further sets of experiments to explore the hypothesis that CFTR indeed mediated Ca^{2+}-regulated chloride secretion. First, we confirmed that ionomycin indeed raised intracellular Ca^{2+} ($[Ca^{2+}]_i$) similarly in normal human AT2 cells (Fig. 4*B*). Second, we performed semi-quantitative PCR analysis in freshly isolated, day 5 and 14 AT2 cells to identify expression of candidate Ca^{2+}-regulated Cl^- channels (Fig. 4*C*). CFTR was expressed, but no mRNA expression of TMEM16A, CLC2, or SLC26A9 was detected in AT2 cells. Moreover, no full-length Bestrophin-1 mRNA expression was detected. Collectively, these data suggest that AT2 cells secrete Cl^- via CFTR in response to $[Ca^{2+}]_i$ signaling in the absence of known CaCC channel expression.

Extracellular Nucleotide-dependent Regulation of Ion Transport in AT2 Cells—Luminal extracellular mediators, *e.g.* triphosphate nucleotides (UTP or ATP) and the adenine nucleoside, adenosine, have been shown to inhibit Na^+ transport and accelerate Cl^- secretion in normal airway epithelial cells (17). To test whether a similar physiology exists in the alveolar epithelium, normal human AT2 cultures were exposed to UTP (100 μM, luminal) under basal conditions. A rapid increase in PD was observed followed by a small consistent later reduction in PD (Fig. 5*A*). I_{eq} analyses revealed that UTP stimulated an approximate 17 $\mu A/cm^2$ increase in current that reflected anion (Cl^-) secretion (Fig. 5*B*, *UTP (early)*), followed by an inhibition of I_{eq}, likely reflecting inhibition of Na^+ absorption (Fig. 5*B*, *UTP (late)*).

Next, we exposed human AT2 cells to UTP in the presence of amiloride (Fig. 5*C*). The increase in I_{eq} was ~20 $\mu A/cm^2$. Similar to ionomycin, the UTP-stimulated Cl^- secretion in normal AT2 cells was significantly reduced in the presence of $CFTR_{inh}$-172 (Fig. 5, *D* and *E*). As with ionomycin, we verified with fura-2 measurements that UTP raised intracellular Ca^{2+}. These data suggest that the nucleotide-regulated anion secretion reflects Ca^{2+} activation of CFTR.

We next characterized the relative efficacy for Cl^- secretion of purinoceptor agonists by exposing normal AT2 cultures to ATP, adenosine, or UDP in the presence of amiloride (Fig. 5*G*). Although all agonists stimulated increases in ΔI_{eq}, the response to ATP was smaller when compared with UTP (Fig. 5, compare *E* and *G*). The UDP and adenosine responses were both small relative to UTP/ATP.

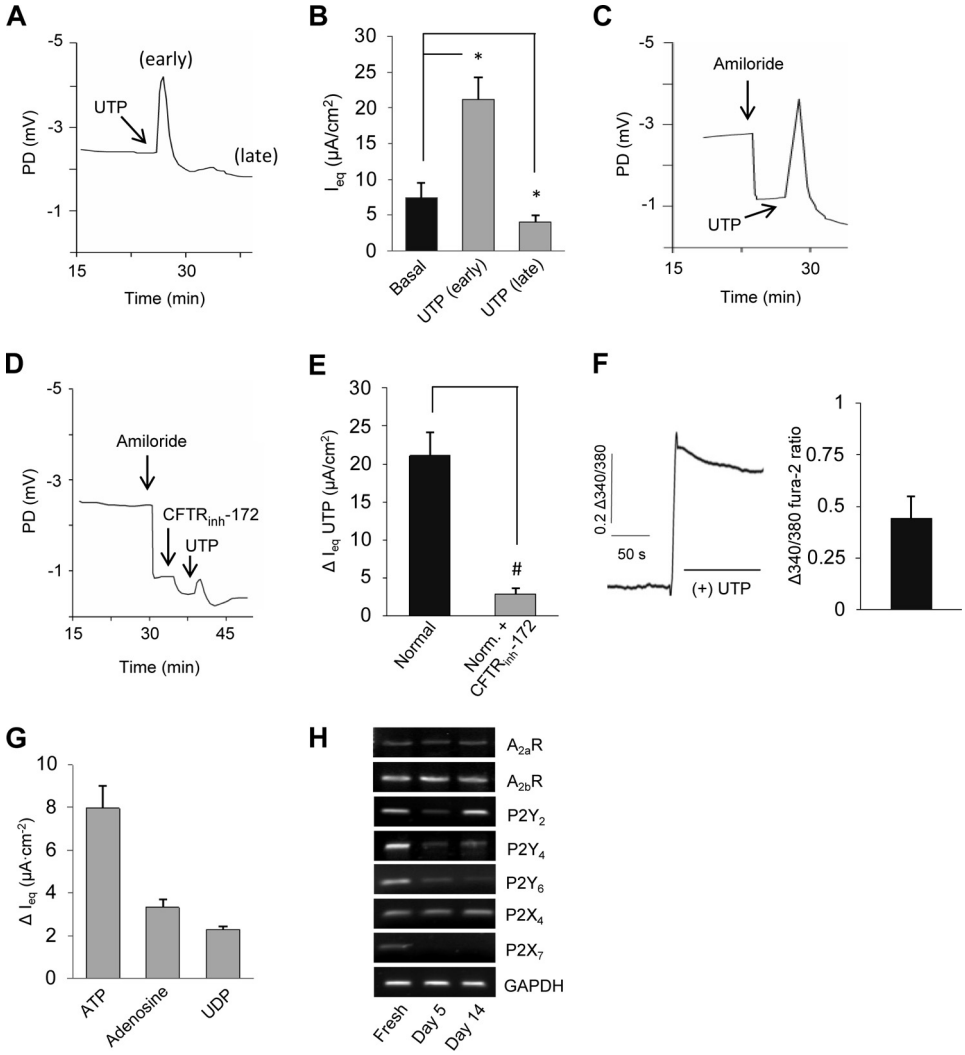

FIGURE 5. **Nucleotide/nucleoside-mediated regulation of human AT2 cell ion transport.** *A*, potential differences were measured in normal AT2 cultures before and after exposure to UTP (100 μM, luminal) in Ussing chambers. *B*, the "early" and "late" responses to UTP were quantitated. Summary data describing equivalent short circuit current (I_{eq}) in normal AT2 cells before and after (early/late) UTP exposure (means ± S.D.; $n \geq 6$; *, $p < 0.05$). *C* and *D*, UTP effect on potential differences in amiloride-pretreated normal AT2 cultures (*C*) and normal AT2 cultures treated with CFTR$_{inh}$-172 (*D*). *E*, changes in equivalent short circuit current for UTP responses without and with CFTR$_{inh}$-172 pretreatment conditions (means ± S.D.; $n \geq 6$; #, $p < 0.01$). *F*, Ca^{2+} mobilization (Δ340/380 fura-2 ratio) was measured in normal AT2 cultures following the addition of UTP (100 μM, luminal). *G*, ATP (100 μM), adenosine (100 μM), or UDP (100 μM) was added apically to normal AT2 cultures, and ΔI_{eq} was measured and summarized (mean ± S.D.; $n \geq 3$). *H*, semi-quantitative PCR analysis to identify gene expression of nucleotide/nucleoside purinergic receptors present in normal AT2 cells freshly isolated and over time in culture.

To identify which receptors may be transducing nucleotide/nucleoside responses, semi-quantitative PCR was performed for nucleotide (P2Xs/P2Ys) and adenosine receptors expressed in either freshly isolated, day 5 in culture, or day 14 post-seeding AT2 cells. The $A_{2a}R$ and $A_{2b}R$ adenosine receptors were expressed in freshly isolated cells and cultured AT2 cells (Fig. 5*H*). $P2Y_2$, $P2Y_4$, and $P2Y_6$ were all expressed in fresh isolates, as well as within cultures seeded for 5 or 14 days (Fig. 5*H*). The $P2X_4$ receptor was present throughout all time periods, whereas $P2X_7$ was only present in freshly isolated cells.

Regulation of AvSL by AT2 Cultures—We first asked whether AT2 cell cultures homeostatically regulated surface liquid volume in response to a liquid challenge, similar to airway epithelia (17). Confluent live AT2 cells were stained using Celltrace™ Calcein Green, followed by the addition of 25 μl of PBS containing a Texas Red-labeled 70-kDa dextran fluorescent probe to the culture surface. AvSL height was then quantitated for 24 h by confocal microscopy (Fig. 6, *A* and *B*). A rapid decrease in AvSL height was observed after "flooding" the cultures, following which a steady state height was achieved at ~4–5 μm.

In airway epithelial cells, the steady state ASL height is determined by the rates of nucleotide release and the ASL nucleotide/nucleoside concentrations that result (18). Using the luciferin/luciferase assay, we measured basal ATP concentrations in the AvSL covering AT2 cultures and found it to be 8.0 ± 4.2 nM (Fig. 6*C*). The basal ATP concentration reflects the balance between the rate of ATP release (891.9 ± 300.0 fmol/cm^2/min; Fig. 6*C*) and ecto-metabolism (36). To explore the role of nucleotide release/basal concentrations in regulating basal AvSL height, we measured AvSL height in untreated AT2 cultures *versus* those treated with an enzyme, apyrase (10 units/ml), on the apical surface that metabolizes all nucleotides in the local environment. Untreated normal human AT2 cultures exhibited persistent AvSL heights of ~4–5 μm over 4 h, whereas cultures treated with apical apyrase absorbed virtually all AvSL (Fig. 6, *D* and *E*). Thus, we conclude that basal AvSL height is dependent on AvSL nucleotide concentrations.

We next explored mechanisms that might regulate liquid transport in normal AT2 cultures. To perform these experiments, we started each protocol with a relatively thin film of AvSL to simulate *in vivo* conditions (Fig. 7*A*). In control experiments, the residual liquid was absorbed over time, reaching a steady state height again of ~4–5 μm (Fig. 7*A*). We first investigated the contribution of the cAMP-releasing agent forskolin to AvSL height regulation. Surprisingly, unlike the forskolin-mediated increase in Na^+ absorption observed in Ussing chambers (Fig. 2, *F* and *H*), forskolin stimulated an increase in AvSL height, *i.e.* liquid secretion, within 30 min of treatment, followed by a return to basal liquid height by 4 h (Fig. 7, *A* and *B*). To test whether CFTR mediated the liquid secretion in response to forskolin addition, normal AT2 cultures were pretreated with CFTR$_{inh}$-172 for 30 min followed by the addition of forskolin.

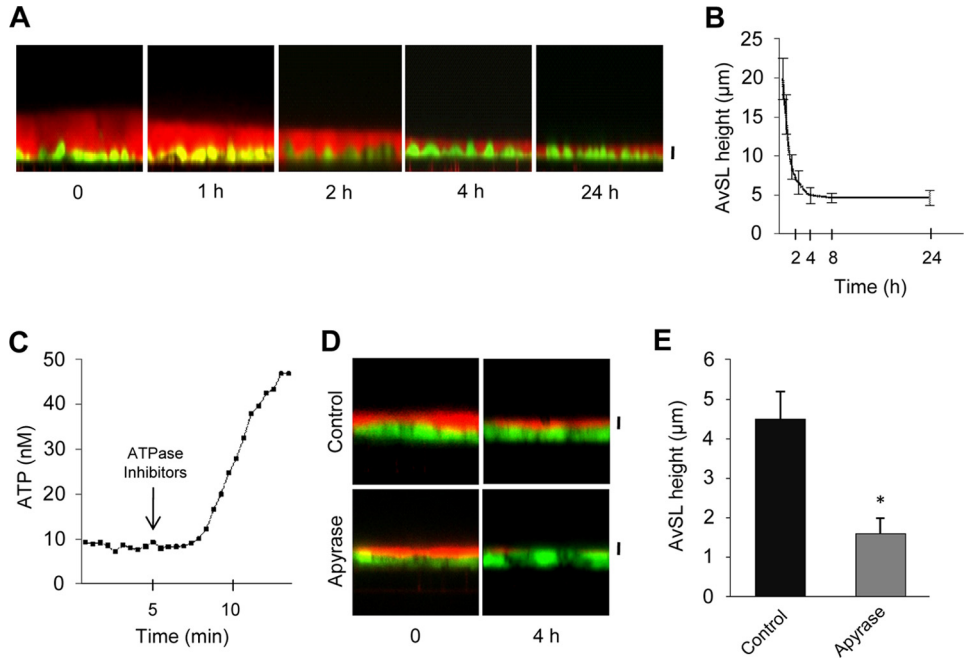

FIGURE 6. **Regulation of basal AvSL height by normal human AT2 cultures.** Live human AT2 cells were labeled with Calcein Green, and then the AvSL was labeled with a Texas Red-labeled 70-kDa dextran fluorophore. *A*, AvSL height was measured serially after the addition of the Texas Red-labeled 70-kDa dextran fluorophore (25 μl) by confocal microscopy. *B*, the mean changes in AvSL height were measured and plotted over 24 h. *C*, luminal extracellular ATP levels were measured in normal AT2 cultures using the luciferase/luciferin assay in the absence (basal levels) and presence of ATPase inhibitors (measure of ATP release rate). *D*, AvSL height was imaged by confocal microscopy over 4 h in the absence or presence of apyrase (10 units/ml). *E*, AvSL height was quantitated at 4 h before and after apyrase treatment (mean ± S.D.; $n \geq 3$; *, $p < 0.05$). All of the original images were *z* scans taken using a 63× objective. All of the *scale bars* represent 5 μm.

The forskolin-induced increase in AvSL height was significantly reduced in the presence of $CFTR_{inh}$-172 (Fig. 7*B*). These findings suggest that forskolin-induced liquid secretion is highly CFTR-dependent in human AT2 cells.

The disparity in the directionality of responses to forskolin in AT2 cultures in the Ussing chamber (absorption) *versus* confocal measurements (secretion) likely reflects differences in the conditions of the two assays. The Ussing chamber's large bathing volumes "dilute" signals within AvSL (*e.g.* nucleotides) that accumulate within the thin film liquid conditions reprised in the confocal technique. For forskolin to elicit secretion under thin film conditions, such "signals" in AvSL would need to inhibit ENaC sufficiently to generate an electrochemical gradient for Cl^- secretion and block forskolin-mediated ENaC activation. Candidate endogenous signals that inhibit ENaC are the tri-phosphate nucleotides, *e.g.* ATP or UTP.

Direct measurements of ATP on the apical surface of AT2 cells suggested that the basal concentration was ~8 nM. It is not clear that this concentration alone is sufficient to inhibit ENaC and generate the driving forces for forskolin-dependent Cl^-/liquid secretion. Therefore, we speculated that forskolin may also stimulate nucleotide release (ATP) to further inhibit ENaC and promote a secretory response. Measurements that detected an increase in ATP release rates induced by forskolin were consistent with this notion (Fig. 7*C*).

Finally, we asked whether nucleotides in AvSL were required to produce the forskolin-induced secretory response. To address this question, we again used the strategy of including apyrase in the luminal surface liquid to metabolize released nucleotides. Importantly, pretreatment of the AvSL with apyrase markedly blunted the volume secretory response to forskolin (Fig. 7, *D* and *E*), suggesting a requirement for nucleotides in the forskolin-mediated AT2 cell secretory response.

Regulation of AvSL Height by Cyclic Compressive Stress/Nucleotide Release—Because it has been previously shown in airway epithelial cultures that ASL height is regulated by mechanical stresses that mimic normal tidal breathing (21) via regulation of nucleotide release rates, we asked whether a similar physiology exists in AT2 cells. First, the role of nucleotides in mediating the CCS response was explored in studies of nucleotide regulation of AvSL volume. Luminal UTP (100 μM) addition stimulated AT2 cell liquid secretion within 30 min, returning to the basal 4–5-μm height within the 4-h observational interval (Fig. 8*A*). Similar to forskolin, the rapid UTP volume secretory response was significantly blocked by pretreatment with $CFTR_{inh}$-172 (Fig. 8*B*). Second, AT2 cultures were subjected to CCS for 24 h, and the change in AvSL height was measured. Normal AT2 cultures demonstrated a significant increase in AvSL height 3 h after exposure to CCS, and the AvSL height was increased further at 24 h of continuous CCS exposure (Fig. 8*C*), demonstrating that CCS stimulated liquid secretion in AT2 cultures. AvSL liquid secretion was markedly inhibited in cultures pretreated with apyrase (Fig. 8*D*), demonstrating a nucleotide-mediated regulation of AvSL height under CCS conditions.

DISCUSSION

A balance sheet describing the integrated homeostasis of secretion, absorption, and surface movement of liquids on pulmonary surfaces has remained elusive. Whereas it is clear that liquids move cephalad along airway surfaces via the actions of cilia and potentially gas-liquid pumping (2), the origin of airway surface liquids is unclear. Two sites of secretion appear plausible. First, it is possible that secretions are formed by active ion transport mechanisms on distal small airway surfaces, although studies of ion transport gene expression and function do not support such a notion (37–39). Alternatively, active ion secretion by alveolar surfaces could mediate liquid secretion with movement of secreted liquids onto small airway surfaces. However, despite some recent evidence for this latter notion (16, 40), the prevailing concept has been that the alveolus is primarily absorptive (41–43).

The ideal approach to this question is to study the intact alveolar epithelium; however, this approach is difficult because of the anatomy of the airway. Although it is likely that AT1 cells

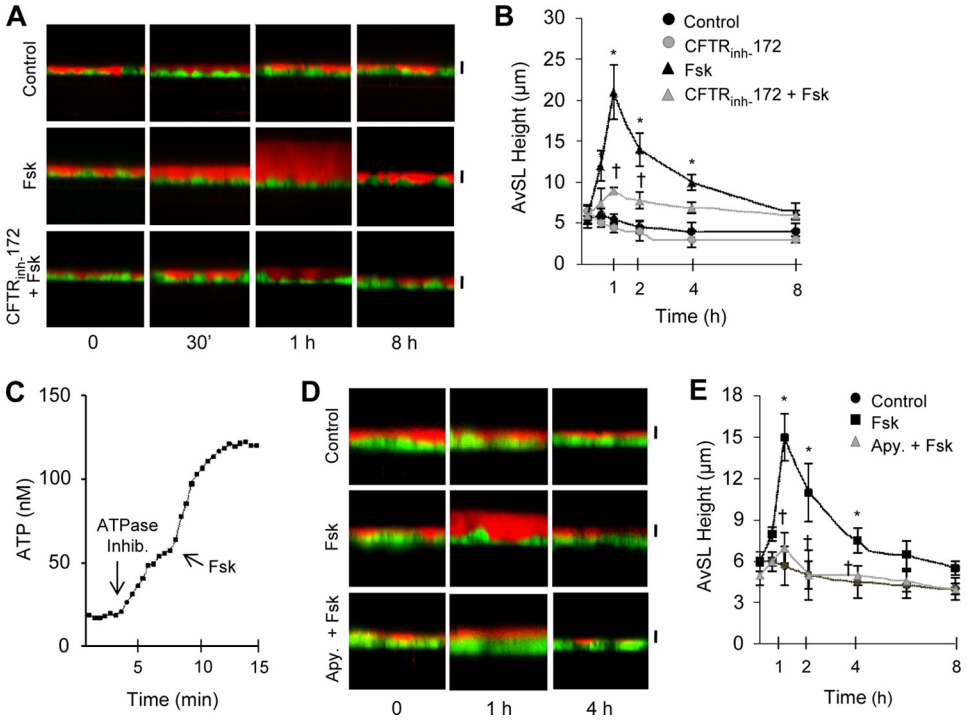

FIGURE 7. **Regulation of AvSL height by forskolin by normal human AT2 cultures.** Normal human AT2 cells were labeled with Calcein Green, and AvSL was labeled with 25 μl of Texas Red-labeled 70-kDa dextran fluorophore for 30 min prior to aspiration. *A*, control and post-forskolin AvSL height starting from basal thin film conditions were imaged by confocal microscopy in confluent normal AT2 cultures over 8 h. *B*, confluent normal AT2 cultures were treated without (control) or with forskolin, in the absence or presence of $CFTR_{inh}$-172, and AvSL height was measured over 8 h (mean ± S.D.; $n \geq 3$; *, $p < 0.05$ different from control; †, $p < 0.05$ different from forskolin (*Fsk*) treatment). *C*, luminal ATP release rates were measured before and after exposure to forskolin (10 μM) in the continued presence of ATPase inhibitors. *D*, confocal images showing control, forskolin (10 μM), and apyrase (10 units/ml)/forskolin-treated normal AT2 cells. *E*, summary data plotting AvSL height *versus* time in control, forskolin-treated, and apyrase/forskolin-treated normal AT2 cultures (means ± S.D.; $n \geq 3$; *, $p < 0.05$ different from control; †, $p < 0.05$ different from forskolin treatment). All of the *scale bars* represent 5 μm.

have the capacity and machinery for active ion transport, currently no AT1-derived cell culture model has been successfully developed to study ion/liquid transport properties on a confluent AT1 monolayer. Therefore, like others, we focused on studying this question in isolated and cultured human AT2 cells. Our data suggest that they form moderate resistance (~400 Ω*cm^2) monolayers with basal short circuit currents of ~7 $\mu A/cm^2$. Approximately 60% of the basal current was sensitive to the Na^+ transport inhibitor amiloride. Less than 5% of basal I_{sc} was sensitive to the inhibitor of CFTR-mediated Cl^- secretion, $CFTR_{inh}$-172. Thus, basal ion transport of human AT2 cells in Ussing chambers, in which the lumen is flooded and endogenous surface liquid signals/regulators are diluted, is dominated by Na^+ absorption.

We next studied the mechanisms mediating Na^+ transport in cultured human AT2 cells. As noted above, Na^+ absorption was inhibited by the ENaC blocker, amiloride, with a K_i of ~5×10^{-7} M (Fig. 2*D*). The subunit composition of ENaC determines the amiloride K_i and can vary among tissues. Our data, with respect to ENaC subunit mRNA expression in AT2 cells, suggest that ENaC is comprised potentially of α, β, and γ ENaC, but not δ ENaC (Fig. 2*A*). The amiloride K_i for Na^+ transport inhibition by amiloride in AT2 cells is shifted by approximately 1 order of magnitude to the right from that reported for α, β, and γ channels expressed heterologously in oocytes (44). ENaC channels composed of $\alpha\alpha\alpha$ENaC subunits or $\alpha\beta$ subunits expressed in oocytes exhibit amiloride K_i values similarly shifted to the right (7). Thus, it is possible that Na^+ transport in AT2 cells is mediated by a combination of ENaC channels with different stoichiometries, *e.g.* $\alpha\beta\gamma$ and $\alpha\alpha\alpha$, as has been suggested by the patch clamp data of Eaton *et al.* (7). Note that we found relatively little evidence for a large contribution of other Na^+ transport processes to AT2 cell Na^+ transport, including electrogenic Na^+-glucose transport, Na^+-amino acid transport, or cyclic nucleotide-gated cation channel-mediated transport.

The regulation of Na^+ transport rates in normal AT2 cells appears to be quite distinct from that in airway epithelial cells. For example, the addition of agents that raise intracellular cAMP, *e.g.* forskolin, raised Na^+ transport rates in normal AT2 cells (45) (Fig. 2*E*), whereas these agents inhibit Na^+ transport in airway epithelial cells (46). The cAMP-dependent inhibition of ENaC activity in airway epithelia has been attributed to CFTR, based on studies in heterologous cells that demonstrated cAMP-dependent, CFTR-mediated inhibition of ENaC (47–49). Thus, the observation that forskolin raises AT2 cell Na^+ transport rates in normal AT2 cells suggests that CFTR does not have an inhibitory role in ENaC function in this cell type.

With respect to Cl^- transport, airway Cl^- secretion is dominated in the submucosal gland acini by CaCC activities, whereas in the superficial epithelium Cl^- transport is mediated by both CFTR and CaCC (50, 51). In striking contrast, it appears that CFTR is the principal Cl^- channel mediating Cl^- secretion in normal human AT2 cells, with little evidence for CaCC expression/function. For example, agents that raise intracellular cAMP, *e.g.* forskolin, activated normal AT2 cell anion secretory currents that were inhibited by $CFTR_{inh}$-172. Ionomycin (Fig. 4, *A* and *B*) or luminal nucleotides (Fig. 5*C*), *e.g.* ATP or UTP, also activated Cl^- secretory currents in normal AT2 cells. However, in contrast to airway cells, the stimulated secretory currents were inhibited by $CFTR_{inh}$-172, implying that they were mediated by CFTR and not CaCC. The failure of ionomycin or UTP to activate CaCC was not due to failure to raise $[Ca^{2+}]_i$, as evidenced by the large $[Ca^{2+}]_i$ responses to ionomycin or UTP (Figs. 4*B* and 5*F*). Indeed, our data suggest that the failure to activate CaCC-mediated currents by ionomycin or UTP reflects the virtual absence of expression of some known CaCC channels in human AT2 cells, including TMEM16A, ClC2, SLC26A9, and Bestrophin-1 (Fig. 4*C*).

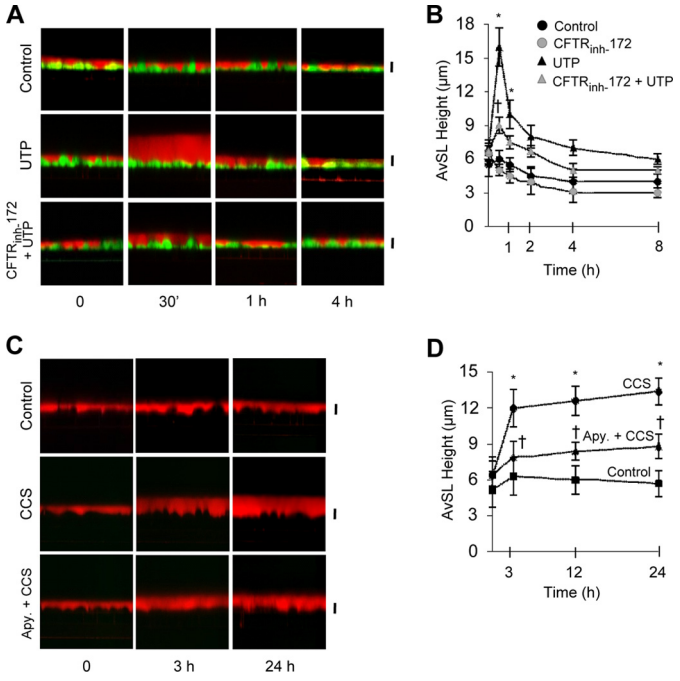

FIGURE 8. **Cyclic compressive stress/nucleotide regulation of AvSL height of normal human AT2 cultures.** Normal human AT2 cells were labeled with Calcein Green, and AvSL was labeled with (25 μl) Texas Red-labeled 70-kDa dextran fluorophore for 30 min and then aspirated. *A*, control and post-UTP addition (100 μM, luminal) in AvSL heights were imaged by confocal microscopy in confluent normal AT2 cultures. *B*, confluent normal AT2 cultures were treated without (*Control*) or with UTP in the absence or presence of CFTR$_{inh}$-172, and AvSL height was measured (mean ± S.D.; $n \geq 3$; *, $p < 0.05$ different from control; †, $p < 0.05$ different from UTP treatment). *C*, normal human AT2 cultures were subjected to constant CCS (0–20 cm H_20) for 24 h, and AvSL height was imaged using confocal microscopy. *D*, summary data for normal AT2 cultures exposed to control (static) conditions and CCS for 24 h without (*Control*) or with apyrase (*Apy.*, 10 units/ml) treatment (means ± S.D.; $n \geq 3$; *, $p < 0.05$ different from control; †, $p < 0.05$ different from CCS). All of the *scale bars* represent 5 μm. (Basolateral fluorescence occurs if minor disruption occurs in the seal between the cell monolayer and the Transwell membrane. This event occurs rarely and does not affect the overall integrity of the experiment.)

The observation that CFTR is the principal anion channel in the apical membrane of human AT2 cells raises two questions. First, if nucleotides do not regulate CaCC by Ca^{2+} signaling, how do they regulate CFTR activity? It is possible that the raised Ca^{2+} levels associated with nucleotide receptor activation couple with diacylglycerol formation and adenyl cyclases activate PKC and CFTR (52, 53). However, it should also be noted that Kunzelmann and co-workers (54) recently suggested a non-PKC-dependent mechanism for nucleotide regulation of CFTR via as-yet-unknown protein phosphatase(s). The second important question is, why do CF patients not experience more alveolar disease, if indeed CFTR is the sole anion channel in the apical membrane of CF cells? The answer to this question will await a more complete characterization of potential other anion channels in CF cells and further elucidation of the normal ion/liquid transport physiology of the alveolus *in vivo*.

A series of studies have demonstrated the importance of nucleotide/nucleoside concentrations in airway surface liquid in directing the relative rates of absorption *versus* secretion across human airway epithelial barriers (17, 21). A complex but somewhat different physiology is evident in our studies of AT2 transport function. For example, nucleotides exhibit the capacity to inhibit ENaC activity and, as noted above, also to accelerate anion secretion. Nucleotide regulation of K^+ secretion is likely as well but is not investigated in these studies. As reported for alveolar epithelia from rat, a large number of purinoceptors are potentially expressed on the apical membrane of human AT2 cells. Like airways, the $P2Y_2$-R triphosphate nucleotide receptor (recognizing ATP and UTP) and the UDP liganded $P2Y_6$ receptor, are expressed and appear functional in human AT2 cells. Of note, the anion secretion activated by UTP (Fig. 5, *C* and *E*) is larger than that activated by ATP (Fig. 5*G*) in AT2 cells. This observation suggests that the UTP selective $P2Y_4$ and not the ATP-ligand $P2X_4$ or P2Y2 receptors may be the dominant nucleotide receptor on the apical membrane of AT2 cells. Of note, Matalon and co-workers (55) have suggested in mouse models that the release of UTP in the distal lung in response to viral infection can produce a secretory pulmonary edema. Finally, in the presence of amiloride, adenosine was active in initiating anion secretion, likely through an A_{2b} receptor, but this secretion is smaller than activated by triphosphate nucleotides. Again, Matalon and co-workers (12) have suggested a role for adenosine in mediating secretion in the murine alveolus.

It has been difficult to achieve a unified understanding of the surface liquid physiology of the intact alveolus. A first study to explore AT2 liquid homeostatic capabilities with the confocal microscopy technique was to place a small volume of liquid on the AT2 culture surface and observe how the epithelium responded to this challenge. As shown in Fig. 6*A*, when the AT2 cell surface was effectively flooded by this maneuver, the AT2 cells absorbed the added liquid over a 2–4-h period, following which AT2 cells appeared to balance absorption and secretion to maintain a steady state surface liquid height of ~4–5 μm.

This simple experiment has two implications. First, it appears that when signals that are contained within the AT2 cell surface liquid are diluted by exogenous liquid addition, the AT2 cells revert to an absorptive mode. These data are consistent both with a response of human airway epithelial culture to similar maneuvers and, indeed, with observations that the mammalian alveolus *in vivo*, when flooded, exhibits a volume-absorptive phenotype (41, 56, 57). Second, the AT2 cell preparations generated a steady state surface liquid height of ~4–5 μm. In airway epithelia devoid of cilia, an airway surface liquid height of 4–5 μm in steady state is also maintained, in large part reflecting the rate ATP secretion and ATP/ADO regulation of Na^+ *versus* Cl^- transport to achieve a homeostatic surface liquid level (17). Our data reveal that AT2 cell monolayers: 1) release ATP at a rate somewhat greater than airway epithelial cells (800 fmol/cm^2/min *versus* 300 fmol/cm^2/min (31) (Fig. 6*C*)); 2) produce a resting AvSL ATP concentration (~8 nM) somewhat higher than airway epithelia (Fig. 6*C*); and 3) cannot maintain a basal AvSL height/volume in the presence of apyrase (Fig. 6, *D* and *E*), arguing that the basal AvSL height is, like airway epithelial cells, determined by nucleotide release/signaling.

We also employed the confocal technique to ask how AT2 cell monolayers regulate volume in response to the prototypic regulators of ion transport under basal physiologic thin film conditions. Forskolin, via raised cellular cAMP concentrations, induced volume secretion, not absorption as predicted from

Ussing chamber studies (Fig. 2*F*), under these conditions (Fig. 7, *A* and *B*). Our data suggest that the inhibition of ENaC sufficient to generate electrochemical driving increases for forskolin-stimulated, CFTR-mediated Cl^- secretion was provided by nucleotides in the AvSL (Fig. 7*B*). We speculate that basal ATP release and forskolin-induced ATP release, perhaps as a consequence of secretion of surfactant granules that contain ATP, provided the autocrine nucleotide signal for ENaC inhibition/CFTR activation required to generate cAMP-regulated volume secretion. Note that there has been a perplexing failure of β-agonists to therapeutically accelerate edema absorption in respiratory distress syndrome patients (58). As one explanation, inflammation may reduce β-agonist signaling to account for this therapeutic failure (59). However, our data raise the possibility that release of extracellular ATP in RDS is sufficient to cause β-agonists to promote alveolar secretion in patients with this syndrome, offsetting the desired therapeutic absorptive response (60).

UTP also stimulated volume secretion (Fig. 8, *A* and *B*). This result was more predictable based on Ussing chamber results because UTP inhibited ENaC (Fig. 5*A*, *(late)*) and stimulated CFTR-mediated Cl^- secretion (Fig. 5*C*). The UTP secretory volume flow was more transient than forskolin. It is not yet known whether the difference in the kinetics of volume secretion between these two agonists reflects differences in the signaling pathways or, conceivably, the rapid hydrolysis of the UTP added to the alveolar surface.

Our confocal volume transport measurements suggest that alveolar AT2 cells can, depending on conditions, absorb liquid, secrete liquid, or maintain a homeostatic balance of liquid on the AT2 cell surface at a steady state level. Thus, a key question relates to what might AT2-mediated alveolar liquid transport function be *in vivo* under resting/basal conditions? *In vivo*, the alveolus is exposed to cyclic mechanical forces associated with normal tidal breathing. These forces include changes in the trans-alveolar epithelial pressure as a function of expansion of the chest wall. Indeed, changes in transmural wall pressure *in vitro* mimicking those *in vivo* have been shown to induce surfactant secretion in alveolar epithelia in culture (61) and in human airway epithelia to increase ATP release (18). Recently, it has been shown that increased alveolar pressures also release ATP from the rat and mouse lung *in vivo*, in the context of alveolar-endothelial signaling (62). As shown in Fig. 8*C*, the application of cyclic compressive stress induced sustained liquid secretion that appeared dependent on nucleotide release. Thus, these data predict that the AT2 cells under base-line conditions *in vivo* contribute to barrier secretion rather than absorption.

In summary, we have generated a human AT2 monolayer preparation that is amenable to assay by Ussing chamber and confocal liquid transport techniques. The ion transport properties of human AT2 cells appear to differ dramatically from human airway epithelial cells. For example, Na^+ transport in alveolar epithelial cells is ENaC-mediated but is positively regulated by cell cAMP signaling and not inhibited by CFTR activation. In contrast, AT2 cell anion secretion appears to be dominated by CFTR, with no contribution of CaCC (TMEM16A) channel-like activity. Nucleotide signaling appears to be important in both respiratory epithelial regions, but the alveolus may be dominated more by UTP/$P2Y_4$-R signaling and perhaps $P2X_4$ signaling than airway epithelia. The confocal microscopy studies of liquid transport suggest that the AT2 barrier can respond to ambient needs, *e.g.* can absorb in response to the equivalent of alveolar flooding, but can secrete in response to addition of exogenous secretagogues. Further studies will be required to test this hypothesis and analyze how the integrated system, including AT1 cells, contributes to surface liquid transport regulated in response to physiologic stresses in health and in response to pathophysiologic stresses in disease.

Acknowledgments—We thank the Cystic Fibrosis Center Tissue Culture Core for access to normal and CF human lung tissue for AT2 isolation. We thank the Michael Hooker Microscopy Core and Dr. Robert Tarran for the use of the confocal microscope systems. We thank the Cystic Fibrosis Center Molecular Core for the use of reagents and equipment. Also, thanks to Dr. Brian Button for the use of the CCS system and Lisa Brown for help with preparing the manuscript.

REFERENCES

1. Tarran, R., Button, B., Picher, M., Paradiso, A. M., Ribeiro, C. M., Lazarowski, E. R., Zhang, L., Collins, P. L., Pickles, R. J., Fredberg, J. J., and Boucher, R. C. (2005) *J. Biol. Chem.* **280,** 35751–35759
2. Knowles, M. R., and Boucher, R. C. (2002) *J. Clin. Invest.* **109,** 571–577
3. Matthay, M. A., Robriquet, L., and Fang, X. (2005) *Proc. Am. Thorac. Soc.* **2,** 206–213
4. Mason, R. J. (2006) *Respirology* **11,** S12–S15
5. Dobbs, L. G., and Johnson, M. D. (2007) *Respir. Physiol. Neurobiol.* **159,** 283–300
6. Castranova, V., Rabovsky, J., Tucker, J. H., and Miles, P. R. (1988) *Toxicol. Appl. Pharmacol.* **93,** 472–483
7. Eaton, D. C., Chen, J., Ramosevac, S., Matalon, S., and Jain, L. (2004) *Proc. Am. Thorac. Soc* **1,** 10–16
8. Jain, L. (1999) *Clin. Perinatol.* **26,** 585–599
9. Yue, G., Russell, W. J., Benos, D. J., Jackson, R. M., Olman, M. A., and Matalon, S. (1995) *Proc. Natl. Acad. Sci. U.S.A.* **92,** 8418–8422
10. Factor, P., Saldias, F., Ridge, K., Dumasius, V., Zabner, J., Jaffe, H. A., Blanco, G., Barnard, M., Mercer, R., Perrin, R., and Sznajder, J. I. (1998) *J. Clin. Invest.* **102,** 1421–1430
11. Kim, K. J., Cheek, J. M., and Crandall, E. D. (1991) *Respir Physiol.* **85,** 245–256
12. Factor, P., Mutlu, G. M., Chen, L., Mohameed, J., Akhmedov, A. T., Meng, F. J., Jilling, T., Lewis, E. R., Johnson, M. D., Xu, A., Kass, D., Martino, J. M., Bellmeyer, A., Albazi, J. S., Emala, C., Lee, H. T., Dobbs, L. G., and Matalon, S. (2007) *Proc. Natl. Acad. Sci. U.S.A.* **104,** 4083–4088
13. Fang, X., Fukuda, N., Barbry, P., Sartori, C., Verkman, A. S., and Matthay, M. A. (2002) *J. Gen. Physiol.* **119,** 199–207
14. Fang, X., Song, Y., Hirsch, J., Galietta, L. J., Pedemonte, N., Zemans, R. L., Dolganov, G., Verkman, A. S., and Matthay, M. A. (2006) *Am. J. Physiol. Lung Cell Mol. Physiol.* **290,** L242–L249
15. Leroy, C., Privé, A., Bourret, J. C., Berthiaume, Y., Ferraro, P., and Brochiero, E. (2006) *Am. J. Physiol. Lung Cell Mol. Physiol.* **291,** L1207–L1219
16. Lindert, J., Perlman, C. E., Parthasarathi, K., and Bhattacharya, J. (2007) *Am. J. Respir. Cell Mol. Biol.* **36,** 688–696
17. Tarran, R., Trout, L., Donaldson, S. H., and Boucher, R. C. (2006) *J. Gen. Physiol.* **127,** 591–604
18. Button, B., Picher, M., and Boucher, R. C. (2007) *J. Physiol.* **580,** 577–592
19. Lazarowski, E. R., and Boucher, R. C. (2009) *Curr. Opin. Pharmacol.* **9,** 262–267
20. Rollins, B. M., Burn, M., Coakley, R. D., Chambers, L. A., Hirsh, A. J., Clunes, M. T., Lethem, M. I., Donaldson, S. H., and Tarran, R. (2008) *Am. J. Respir. Cell Mol. Biol.* **39,** 190–197
21. Button, B., and Boucher, R. C. (2008) *Respir. Physiol. Neurobiol.* **163,**

189–201
22. Rice, W. R., Burton, F. M., and Fiedeldey, D. T. (1995) *Am. J. Respir. Cell Mol. Biol.* **12,** 27–32
23. Yang, C., Su, L., Wang, Y., and Liu, L. (2009) *Am. J. Physiol. Lung Cell Mol. Physiol.* **297,** L439–L454
24. Boncoeur, E., Tardif, V., Tessier, M. C., Morneau, F., Lavoie, J., Gendreau-Berthiaume, E., Grygorczyk, R., Dagenais, A., and Berthiaume, Y. (2010) *Am. J. Physiol. Lung Cell Mol. Physiol.* **298,** L417–L426
25. Dobbs, L. G. (1990) *Am. J. Physiol.* **258,** L134–L147
26. Deleted in proof
27. Grubb, B. R., Rogers, T. D., Boucher, R. C., and Ostrowski, L. E. (2009) *Am. J. Physiol. Cell Physiol.* **296,** C1301–C1309
28. Grubb, B. R. (1995) *Am. J. Physiol.* **268,** G505–G513
29. Ribeiro, C. M., Paradiso, A. M., Carew, M. A., Shears, S. B., and Boucher, R. C. (2005) *J. Biol. Chem.* **280,** 10202–10209
30. Ribeiro, C. M., Paradiso, A. M., Schwab, U., Perez-Vilar, J., Jones, L., O'neal, W., and Boucher, R. C. (2005) *J. Biol. Chem.* **280,** 17798–17806
31. Okada, S. F., Nicholas, R. A., Kreda, S. M., Lazarowski, E. R., and Boucher, R. C. (2006) *J. Biol. Chem.* **281,** 22992–23002
32. Roomans, G. M., Kozlova, I., Nilsson, H., Vanthanouvong, V., Button, B., and Tarran, R. (2004) *J. Cyst. Fibros.* **3** (Suppl. 2) 135–139
33. Borok, Z., Liebler, J. M., Lubman, R. L., Foster, M. J., Zhou, B., Li, X., Zabski, S. M., Kim, K. J., and Crandall, E. D. (2002) *Am. J. Physiol. Lung Cell Mol. Physiol.* **282,** L599–L608
34. Lazrak, A., Nielsen, V. G., and Matalon, S. (2000) *Am. J. Physiol. Lung Cell Mol. Physiol.* **278,** L233–L238
35. Thiagarajah, J. R., Song, Y., Haggie, P. M., and Verkman, A. S. (2004) *FASEB J.* **18,** 875–877
36. Zuo, P., Picher, M., Okada, S. F., Lazarowski, E. R., Button, B., Boucher, R. C., and Elston, T. C. (2008) *J. Biol. Chem.* **283,** 26805–26819
37. Inglis, S. K., Corboz, M. R., Taylor, A. E., and Ballard, S. T. (1996) *Am. J. Physiol.* **270,** L289–L297
38. Rochelle, L. G., Li, D. C., Ye, H., Lee, E., Talbot, C. R., and Boucher, R. C. (2000) *Am. J. Physiol. Lung Cell Mol. Physiol.* **279,** L14–L24
39. Blouquit, S., Regnier, A., Dannhoffer, L., Fermanian, C., Naline, E., Boucher, R., and Chinet, T. (2006) *Am. J. Respir. Crit. Care Med.* **174,** 299–305
40. Nielsen, V. G., Duvall, M. D., Baird, M. S., and Matalon, S. (1998) *Am. J. Physiol.* **275,** L1127–L1133
41. Berthiaume, Y., and Matthay, M. A. (2007) *Respir. Physiol. Neurobiol.* **159,** 350–359
42. Eaton, D. C., Helms, M. N., Koval, M., Bao, H. F., and Jain, L. (2009) *Annu. Rev. Physiol.* **71,** 403–423
43. Ingbar, D. H., Bhargava, M., and O'Grady, S. M. (2009) *Am. J. Physiol. Lung Cell Mol. Physiol.* **297,** L813–L815
44. Kellenberger, S., Gautschi, I., Rossier, B. C., and Schild, L. (1998) *J. Clin. Invest.* **101,** 2741–2750
45. Fang, X., Song, Y., Zemans, R., Hirsch, J., and Matthay, M. A. (2004) *Am. J. Physiol. Lung Cell Mol. Physiol.* **287,** L104–L110
46. Boucher, R. C., Stutts, M. J., Knowles, M. R., Cantley, L., and Gatzy, J. T. (1986) *J. Clin. Invest.* **78,** 1245–1252
47. Stutts, M. J., Canessa, C. M., Olsen, J. C., Hamrick, M., Cohn, J. A., Rossier, B. C., and Boucher, R. C. (1995) *Science* **269,** 847–850
48. Yan, W., Samaha, F. F., Ramkumar, M., Kleyman, T. R., and Rubenstein, R. C. (2004) *J. Biol. Chem.* **279,** 23183–23192
49. König, J., Schreiber, R., Voelcker, T., Mall, M., and Kunzelmann, K. (2001) *EMBO Rep.* **2,** 1047–1051
50. Krouse, M. E., Hagiwara, G., Chen, J., Lewiston, N. J., and Wine, J. J. (1989) *Am. J. Physiol.* **257,** C129–C140
51. Boucher, R. C., Cheng, E. H., Paradiso, A. M., Stutts, M. J., Knowles, M. R., and Earp, H. S. (1989) *J. Clin. Invest.* **84,** 1424–1431
52. Reddy, M. M., Quinton, P. M., Haws, C., Wine, J. J., Grygorczyk, R., Tabcharani, J. A., Hanrahan, J. W., Gunderson, K. L., and Kopito, R. R. (1996) *Science* **271,** 1876–1879
53. Namkung, W., Finkbeiner, W. E., and Verkman, A. S. *Mol. Biol. Cell.* **21,** 2639–2648
54. Faria, D., Schreiber, R., and Kunzelmann, K. (2009) *Pflugers Arch.* **457,** 1373–1380
55. Song, W., Liu, G., Bosworth, C. A., Walker, J. R., Megaw, G. A., Lazrak, A., Abraham, E., Sullender, W. M., and Matalon, S. (2009) *J. Biol. Chem.* 284, 7294–7306
56. Matthay, M. A., Folkesson, H. G., and Verkman, A. S. (1996) *Am. J. Physiol.* **270,** L487–L503
57. Folkesson, H. G., Nitenberg, G., Oliver, B. L., Jayr, C., Albertine, K. H., and Matthay, M. A. (1998) *Am. J. Physiol.* **275,** L478–L490
58. Roux, J., Carles, M., Koh, H., Goolaerts, A., Ganter, M. T., Chesebro, B. B., Howard, M., Houseman, B. T., Finkbeiner, W., Shokat, K. M., Paquet, A. C., Matthay, M. A., and Pittet, J. F. (2010) *J. Biol. Chem.* **285,** 4278–4290
59. Calfee, C. S., and Matthay, M. A. (2007) *Chest* **131,** 913–920
60. Rich, P. B., Douillet, C. D., Mahler, S. A., Husain, S. A., and Boucher, R. C. (2003) *J. Trauma* **55,** 290–297
61. Gutierrez, J. A., Suzara, V. V., and Dobbs, L. G. (2003) *Am. J. Respir. Cell Mol. Biol.* **29,** 81–87
62. Kiefmann, R., Islam, M. N., Lindert, J., Parthasarathi, K., and Bhattacharya, J. (2009) *Am. J. Physiol. Lung Cell Mol. Physiol.* **296,** L901–L910